Solid State Ionics 331 (2019) 22–29

Contents lists available at ScienceDirect

Solid State Ionics

journal homepage: www.elsevier.com/locate/ssi

Sintering temperature, excess sodium, and phosphorous dependencies on morphology and ionic conductivity of NASICON $Na_3Zr_2Si_2PO_{12}$

Sumaletha Narayanan[a,b], Samuel Reid[b], Shantel Butler[b], Venkataraman Thangadurai[a,*]

[a] Department of Chemistry, University of Calgary, 2500 University Dr NW, Calgary, Alberta T2N 1N4, Canada
[b] Geometric Energy Corporation, 630 8th Ave SW, Calgary, Alberta T2P 1G6, Canada

ARTICLE INFO

Keywords:
NASICON
$Na_3Zr_2Si_2PO_{12}$
Sintering
Conductivity
Density
Temperature dependence

ABSTRACT

The phase pure NASICON $Na_3Zr_2Si_2PO_{12}$ materials were synthesized through solid-state synthesis method at different temperatures ranging from 1100 to 1280 °C to understand the effect of final sintering temperature on the material properties. The structural and morphological characterizations were carried out using powder X-ray diffraction and scanning electron microscopy. The electrical characterizations were performed using AC impedance spectroscopy. The highest ionic conductivity of 1.13 mS cm^{-1} at 20 °C was observed for the NASICON sample, which was sintered at 1100 °C for 12 h using 10 wt% excess sodium precursor $NaNO_3$. The density of the samples appeared to be similar irrespective of the final sintering temperatures. The decrease in conductivity with increase in sintering temperature might be due to the loss of volatile components at high temperature. It is shown by our systematic studies that adding excess Na content alone, rather than adding excess Na and P contents to compensate for the volatile loss, is ideal in synthesizing dense NASICON materials, while keeping the sintering temperature at 1100 °C for 12 h via the solid-state synthesis method. A promising electrochemical stability was observed during the galvanostatic stripping-platting experiment for one of the compositions. This class of materials forms the basis for a sodium-ion electrolyte for all-solid-state sodium-ion secondary battery.

1. Introduction

Energy demand is ever increasing with the growing population modern lifestyle leads today. Fossil fuels are depleted in large amounts to meet this energy demand which in turn raises CO_2 emissions. A cleaner, more sustainable energy source must be utilized to mitigate the runaway effects we now see in the atmosphere. Rechargeable batteries play important role in energy storage as they effectively store energy from renewable sources and are used on demand. Lithium-ion rechargeable batteries dominate the current market due to their high energy density. However, the high cost, flammability hazards, lack of bioavailability, and harmful environmental impact of discarded lithium-ion batteries presents a major challenge for the sustainable energy industry. From safety concerns to cost and sustainability, it is clear we need a new battery in today's market and society. All-solid-state-batteries are the solution to the safety concerns raised by the use of liquid electrolyte in lithium batteries [1]. Solid-state sodium-ion batteries have become the leading contender in sustainable battery technology due to the abundance of sodium within the Earth's crust, their inexpensive cost, and ability to biodegrade [2–4]. Various solid-state materials have been investigated for their use as an electrolyte for sodium batteries with operating temperatures between 100 and 300 °C including Na-β-alumina and Na_3PS_4 glass [5–7]. However, it is important to have a battery that is operational at room temperature to reduce volatility and complexity of the technology [8,9].

NASICON with stoichiometric formula $Na_3Zr_2Si_2PO_{12}$ is a widely studied sodium-ion conducting material [10–20]. Sodium-ion batteries developed from this class of materials are rechargeable, non-explosive, non-toxic, non-flammable, and compare in efficacy to their lithium counterparts. The NASICON material described in this paper forms a basis for advanced materials with the many applications requiring superionic conductivity and high energy density. It is important to conduct a detailed study on $Na_3Zr_2Si_2PO_{12}$ before implementing this material in energy technologies. Different groups have studied the effects of the preparation method and sintering temperature on the properties of $Na_3Zr_2Si_2PO_{12}$ [18,21–24]. However, a systematic study on the effect of sintering temperature, addition of excess sodium (Na) and phosphorous (P), and excess Na contents on the structural and electrical properties of $Na_3Zr_2Si_2PO_{12}$ has not yet been reported to the best of our knowledge. High temperature sintering is an inevitable stage in solid-state synthesis method and hence, it is important to understand how the addition of excess Na and P or excess Na during the solid-state synthesis

* Corresponding author.
E-mail addresses: sam@geometricenergy.ca (S. Reid), vthangad@ucalgary.ca (V. Thangadurai).

https://doi.org/10.1016/j.ssi.2018.12.003
Received 14 October 2018; Received in revised form 27 November 2018; Accepted 3 December 2018
Available online 29 December 2018
0167-2738/

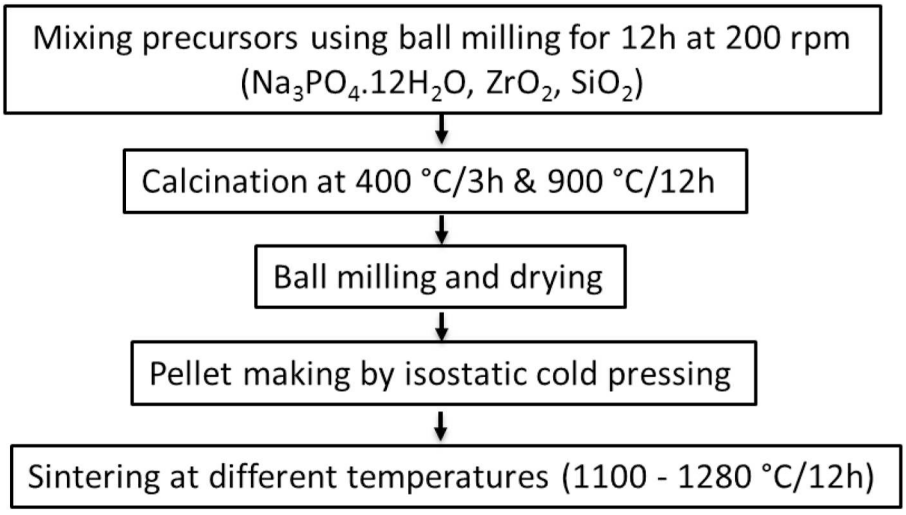

Scheme 1. Solid-state synthesis of $Na_3Zr_2Si_2PO_{12}$.

Table 1
The abbreviation used to represent $Na_3Zr_2Si_2PO_{12}$ samples synthesized at different sintering temperatures with excess Na and P (10 wt% excess $Na_3PO_4{\cdot}12H_2O$) named as NAS1 and excess Na (10 wt% excess $NaNO_3$) named as NAS2.

Sintering temperature (°C)	Sample name	
	$Na_3Zr_2Si_2PO_{12}$ with 10 wt% excess $Na_3PO_4{\cdot}12H_2O$	$Na_3Zr_2Si_2PO_{12}$ with 10 wt% excess $NaNO_3$
1100	NAS1-1100	NAS2-1100
1150	NAS1-1150	NAS2-1150
1200	NAS1-1200	NAS2-1200
1280	NAS1-1280	NAS2-1280

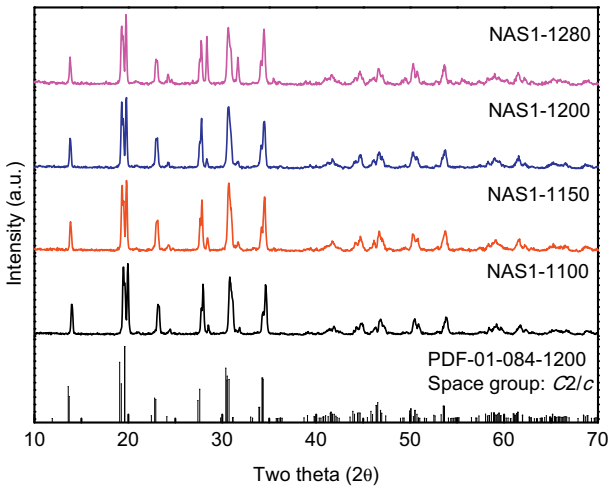

Fig. 1. Powder X-ray diffraction (PXRD) patterns of NASICON $Na_3Zr_2Si_2PO_{12}$ with excess Na and P (NAS1) prepared at different sintering temperatures. The reference XRD pattern of NASICON (PDF no.: 01-084-1200; space group: *C*2/*c*) is provided for the comparison.

method affects the structural and electrical properties. An attempt is made here to study the effect of sintering temperature on the structural and electrical properties of NASICON $Na_3Zr_2Si_2PO_{12}$ material by adding excess Na and P and excess Na alone to the composition.

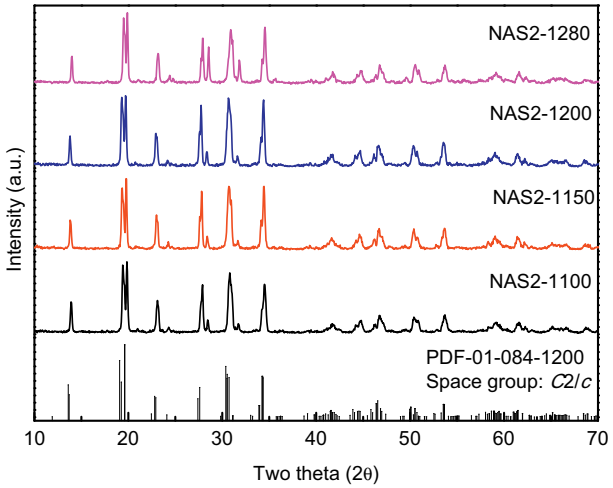

Fig. 2. Powder X-ray diffraction (PXRD) patterns of NASICON $Na_3Zr_2Si_2PO_{12}$ with excess Na (NAS2) prepared at different sintering temperatures. The reference XRD pattern of NASICON (PDF no.: 01-084-1200; space group: *C*2/*c*) is provided for the comparison.

Table 2
The refined lattice parameter (estimated using PROSZKI software) of NAS1 and NAS2 compounds sintered at different temperatures. The reference sued for the calculation was PDF 01-084-1200, monoclinic phase with a space group *C*2/*c* and a = 15.6513 Å, b = 9.055 Å, and c = 9.2198 Å.

NASICON	Lattice parameter (Å)		
	a	*b*	*c*
NAS1-1100	15.581(1)	9.054(4)	9.223(1)
NAS1-1150	15.642(1)	9.049(5)	9.113(1)
NAS1-1200	15.646(3)	9.049(4)	9.144(4)
NAS1-1280	15.765(4)	9.057(7)	9.372(4)
NAS2-1100	15.667 (9)	9.051(4)	9.253(1)
NAS2-1150	15.702(1)	9.004(3)	9.149(7)
NAS2-1200	15.854(1)	9.071(2)	9.077(1)
NAS2-1280	15.561(8)	9.055(3)	9.242(1)

2. Experimental section

2.1. Material synthesis

The NASICON $Na_3Zr_2Si_2PO_{12}$ material was prepared through solid-

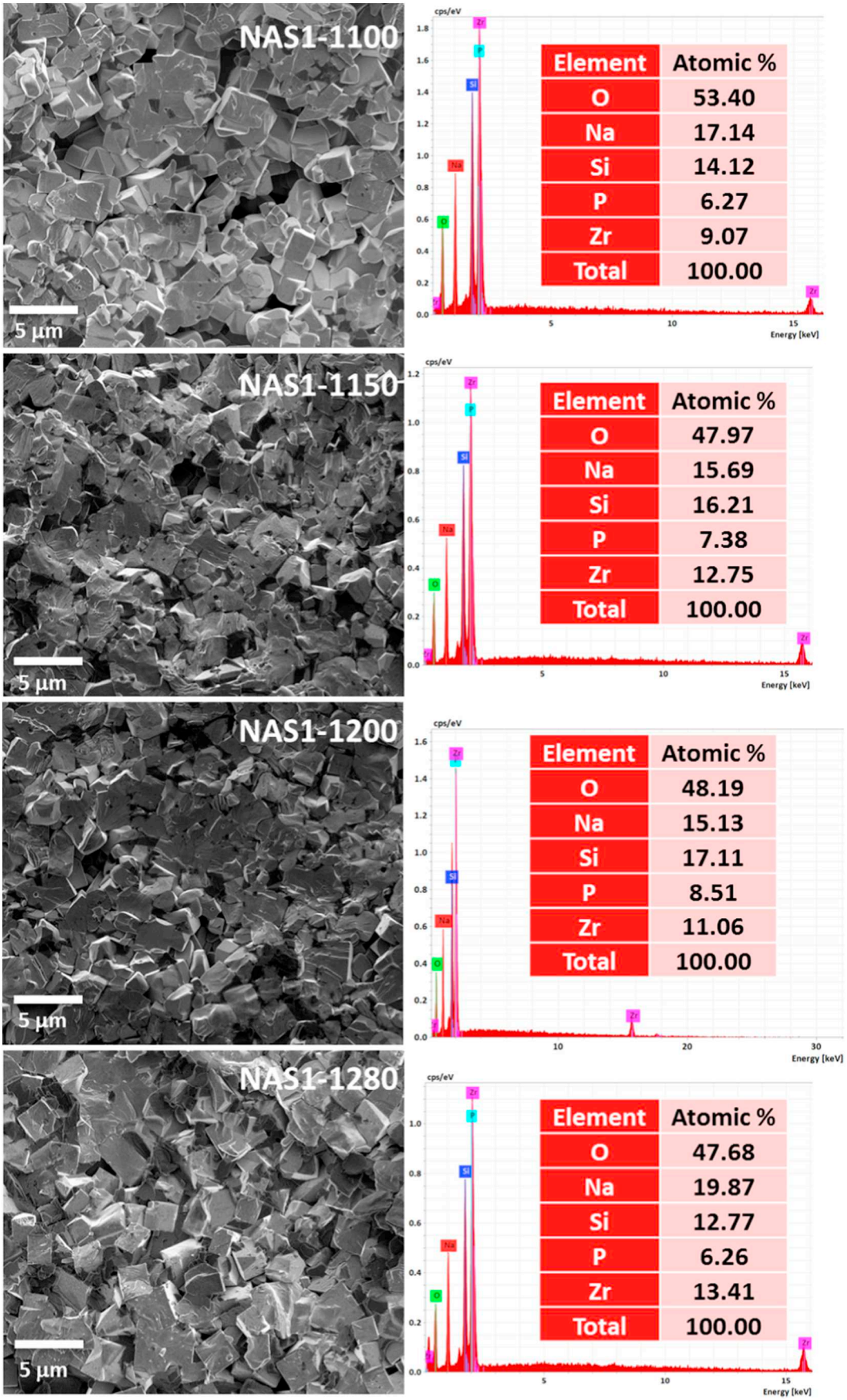

Fig. 3. Scanning electron micrographs (SEM) of $Na_3Zr_2Si_2PO_{12}$ with excess Na and P (NAS1) prepared at different sintering temperatures (1100–1280 °C) in air.

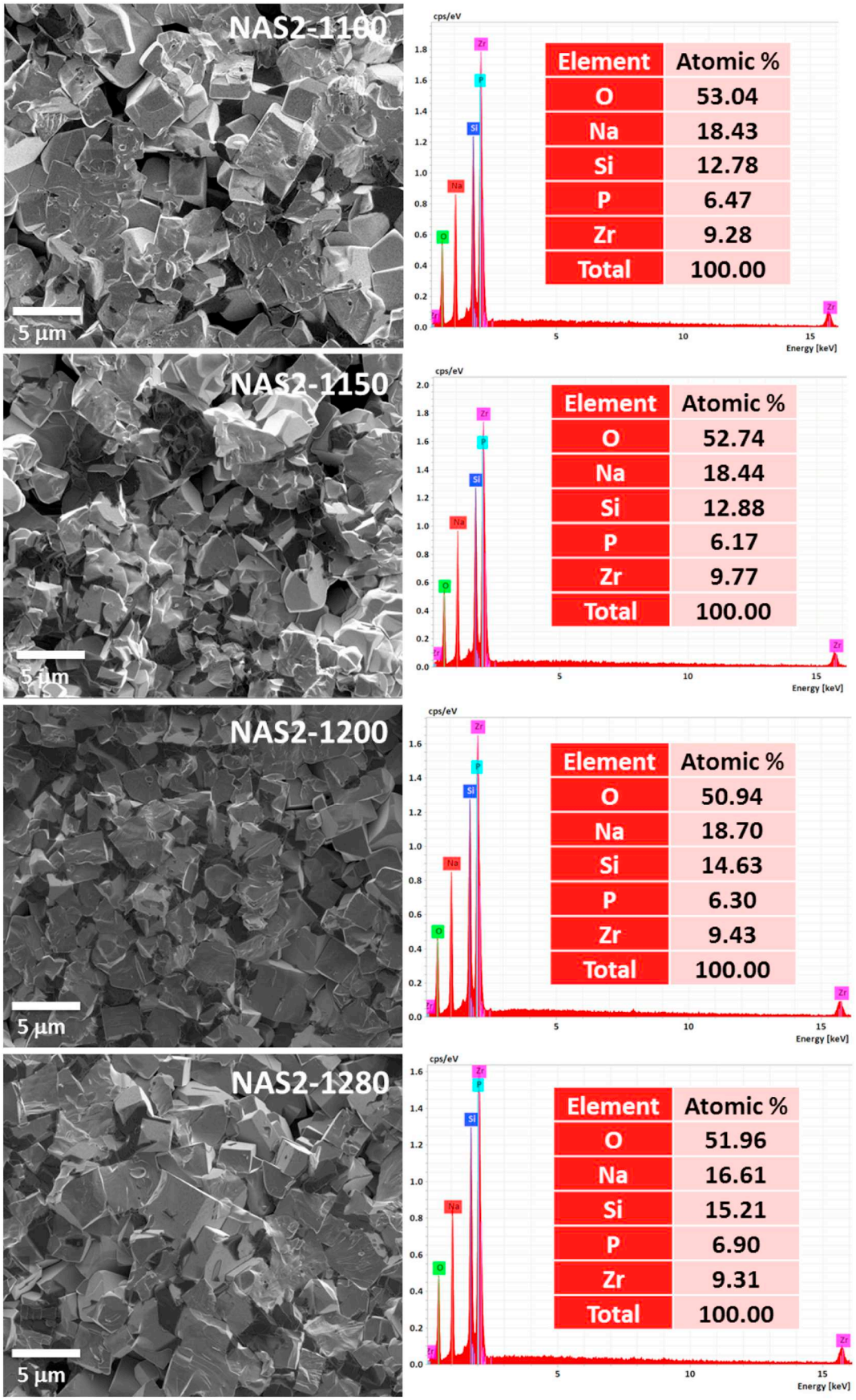

Fig. 4. Scanning electron micrographs (SEM) of $Na_3Zr_2Si_2PO_{12}$ with excess Na (NAS2) prepared at different sintering temperatures (1100–1280 °C) in air.

Table 3
The conductivity at 20 °C, the activation energies calculated at two different temperature ranges 20–180 °C and 200–325 °C using Arrhenius theory (Eq. (2)) and Archimedes density of $Na_3Zr_2Si_2PO_{12}$ samples, NAS1 (with excess Na and P), and NAS2 (excess Na) synthesized at different sintering temperatures.

NASICON	σ at 20 °C (S cm^{-1})	E_a (at 20–180 °C) (eV)	E_a (at 200–325 °C) (eV)	Density (g cm^{-3})
NAS1-1100	3.72×10^{-4}	0.37	0.17	2.761
NAS1-1150	3.86×10^{-4}	0.38	0.20	3.093
NAS1-1200	4.57×10^{-4}	0.36	0.13	3.122
NAS1-1280	9.53×10^{-5}	0.42	0.22	2.938
NAS2-1100	1.13×10^{-3}	0.32	0.13	2.968
NAS2-1150	5.83×10^{-4}	0.35	0.17	2.978
NAS2-1200	3.70×10^{-4}	0.35	0.16	2.954
NAS2-1280	2.46×10^{-4}	0.37	0.15	2.920

state synthesis. The stoichiometric amounts of precursors, $Na_3PO_4{\cdot}12H_2O$ (98–102%, Alfa Aesar), ZrO_2 (99%, Aldrich), SiO_2 (99%, Alfa Aesar) and $NaNO_3$ (98%, Alfa Aesar) were mixed using the high energy ball mill (Pulverisette, Fritsch, Germany) for 6 h at 200 rpm using isopropanol. To compensate for the volatile loss, 10 wt% excess $Na_3PO_4.12H_2O$ or $NaNO_3$ was added to the initial mixture. The resultant powders were heated at 400–900 °C for 12 h to remove the volatiles. Homogeneous mixing was again ensured by ball milling for 6 h at 200 rpm and then the dried powders were used to make pellets using isostatic cold pressing. Final sintering of the pellet samples was carried out in alumina crucibles at elevated temperatures, 1100, 1150, 1200 and 1280 °C for 12 h at a heating rate of 5 °C per minute. The schematic representation of the solid-state synthesis used for this work is provided in Scheme 1. The abbreviation, NAS1 was used for the samples with excess sodium and phosphorus (with 10 wt% excess $Na_3PO_4{\cdot}12H_2O$) and NAS2 was used for the samples with only excess sodium (with 10 wt% excess $NaNO_3$); and the sintering temperature is mentioned along with these abbreviations throughout this paper. For clarity, the sample nomenclature is provided in Table 1.

2.2. Material characterizations

Powder X-ray diffraction (PXRD) was used for the phase analysis of NASICON materials employing Bruker D8 powder X-ray diffractometer (PXRD) with Cu Kα radiation. The morphological analysis was completed using the Field Emission Scanning Electron Microscope (FEI Quanta FEG 37 250). The pellet sample density was measured using Archimedes method and isopropanol was used as the suspension medium. Electrical characterization studies were employed using AC impedance spectroscopy (Solartron SI 1260 impedance and gain-phase analyzer, 0.1 Hz to 1 MHz; 100 mV). Au electrodes were painted on both sides of the pellets and cured at 600 °C for an hour prior to impedance measurements. For the galvanostatic experiment, elemental sodium was rolled and punched on both sides of NASICON pellet and was heated at about 180 °C for 30 min and cooled down to room temperature.

3. Results and discussion

Fig. 1 shows the powder X-ray diffraction (PXRD) patterns of $Na_3Zr_2Si_2PO_{12}$ NASICON with excess Na and P, sintered at different temperatures ranging between 1100 and 1280 °C for 12 h namely, NAS1-1100, NAS1-1150, NAS1-1200, and NAS1-1280 °C. The monoclinic NASICON phase with a space group *C*2/*c* has been formed in all the cases irrespective of the sintering temperature, according to the powder diffraction file (PDF) database number: 01-084-1200 [25]. PXRD patterns of NASICON with excess Na, sintered at different temperatures (NAS2-1100, NAS2-1150, NAS2-1200 and NAS2-1280) also forms the monoclinic phase, as shown in Fig. 2. The lattice parameter calculated using the PROSZKI program is provided in Table 2, which is close to the literature value reported for the monoclinic phase [23,25,26].

Morphology of the NASICON samples was analyzed by scanning electron microscopy (SEM). Figs. 3 and 4 illustrate the SEM micrographs of NAS1 and NAS2 sintered at different temperatures, 1100, 1150, 1200, and 1280 °C as a function of final sintering temperature along with the energy dispersive X-ray spectroscopy (EDX) patterns (right). NAS1-1100 sample looks less dense compared to that of NAS1-1280 sample; however, the density seems to be similar in all the NAS2 samples irrespective of the sintering temperature. The Archimedes density of NASICON materials were measured using isopropanol as the suspension medium and calculated by the equation:

$$D_{Archimedes} = \frac{W_{Dry}}{\left(\frac{W_{Sat} - W_{Susp}}{0.786}\right)} \quad (1)$$

where D is the Archimedes density, W_{Dry}, W_{Sat}, and W_{Susp} are the dry, saturated, and suspended weights, respectively. The denominator indicates the density of isopropanol, 0.786 g cm^{-3}. Table 3 correlates the density and conductivity results of NASICON pellet samples. The density values were found to be comparable to the reported value in literature [14].

Fuentes et al. have found that the density as well as electrical

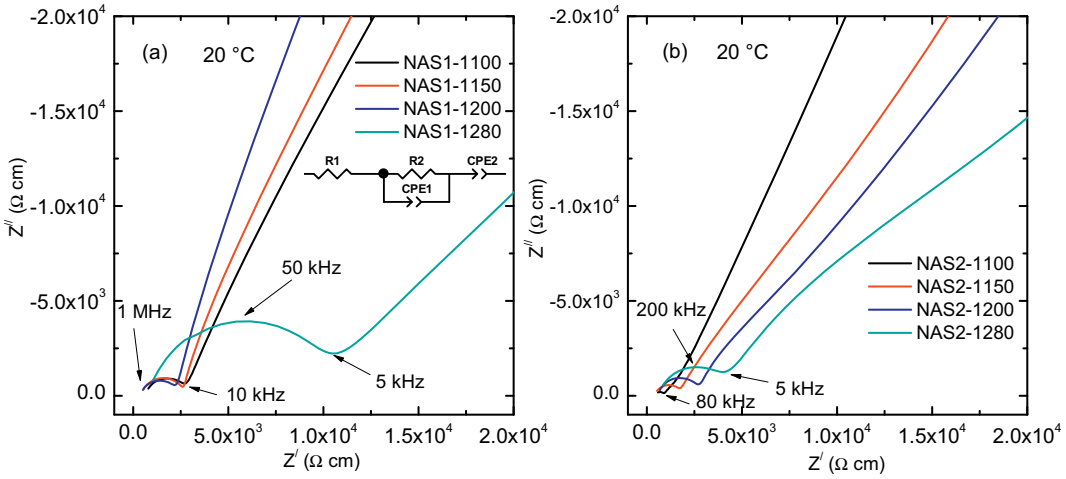

Fig. 5. AC impedance spectra (at 20 °C) of $Na_3Zr_2Si_2PO_{12}$ (a) with excess Na and P (NAS1) and (b) with excess Na prepared at different sintering temperatures, measured in the range of 0.1–1 MHz. Au electrodes which is blocking to Na^+ ions were used on both sides of the NASICON pellets for the impedance measurements.

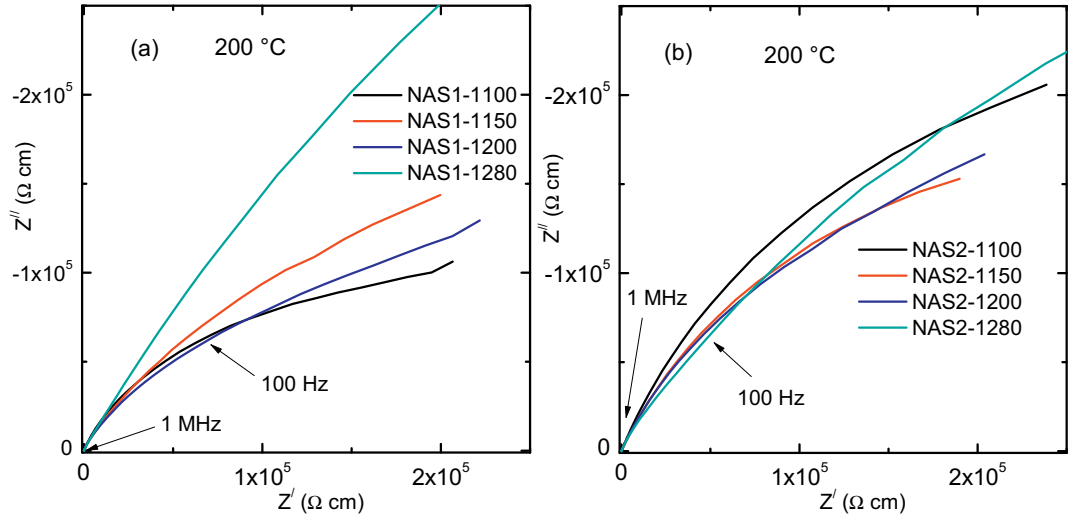

Fig. 6. AC impedance spectra (at 200 °C) of $Na_3Zr_2Si_2PO_{12}$ (a) with excess Na and P (NAS1) and (b) with excess Na prepared at different sintering temperatures, measured in the range of 0.1–1 MHz. Au electrodes which is blocking to Na^+ ions were used on both sides of the NASICON pellets for the impedance measurements.

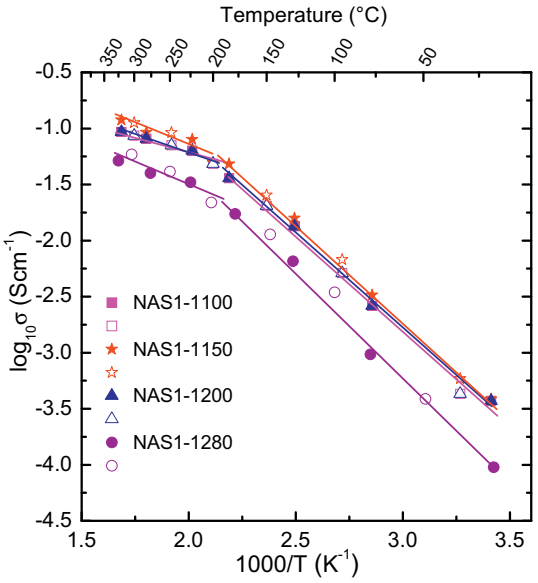

Fig. 7. Arrhenius plots of electrical conductivity of NASICON $Na_3Zr_2Si_2PO_{12}$ with excess Na and P (NAS1) at different sintering temperatures. The solid and open symbols represent the heating and cooling cycles, respectively.

conductivity of NASICON increases by using yttria-stabilized zirconia as a precursor [21]. The density increased with increasing sintering temperatures, which is contradictory to our observations. This may be due to the increased volatilization of Na at higher temperatures, or an unknown effect. From the EDX analysis, it is hard to correlate the composition and the density of NASICON pellets. The $Na_3Zr_2Si_2PO_{12}$ composition is somewhat close to each other in both NAS1 and NAS2 samples.

Electrical characterization of the samples was conducted using AC impedance spectroscopy. The resistivity of NAS1 and NAS2 samples at 20 °C is provided in Fig. 5(a) and (b) as Nyquist plots and the equivalent circuit used for fitting is shown as inset. A semi- circle at the higher frequency side and a tail at the lower frequency side were observed in all cases. The semicircle indicates the grain boundary contribution whereas the tail indicates the blocking electrode nature of Au against Na^+ ions. The resistance at the high frequency intercept to y-axis is considered for the conductivity (s) calculation, using the equation:

$$\sigma = \left(\frac{1}{R}\right)\left(\frac{l}{a}\right) \quad (2)$$

where R is the resistance, l is the thickness of the sample and a is the area of the electrode. The NAS1-1100, NAS-1150, and NAS1-1200 samples show similar and lower resistivity compared to the NAS1-1280 sample. However, the resistivity followed an increasing trend for NAS2 samples with respect to sintering temperature. The NAS2-1100 and NAS2-1280 showed the least and highest resistivity respectively, in the series. At high temperatures, the resistivity plots of both NAS1 and NAS2 show just a spike and such an example at 200 °C is shown in Fig. 6(a) and (b). In these cases, resistance at the first data point just above the x-axis is chosen for the conductivity calculations.

The conductivity of the NAS1 and NAS2 NASICONs sintered at different temperatures are represented in Figs. 7 and 8 and the activation energy for electrical conductivity was estimated using the Arrhenius equation (Eq. (3)),

$$\sigma T = A\exp\left(\frac{-E_a}{kT}\right) \quad (3)$$

where A is the pre-exponential factor, E_a is the activation energy, T is the temperature, and k is the Boltzmann constant (1.38×10^{-23} J K^{-1}). The conductivity of the NAS1-1100, NAS1-1150, and NAS1-1200 samples are very close throughout the measured temperature range of 20–325 °C. The room temperature (20 °C) conductivity is in the order of 10^{-4} S cm^{-1}. The conductivity of high temperature sintered NAS1-1280 showed about half an order of magnitude less conductivity than that of the other samples which were sintered at lower temperatures. Among the NAS2 samples, NAS2-1100 showed the best room temperature Na ion conductivity of 1.13 mS cm^{-1} and the conductivity decreased upon increasing the sintering temperature. It was observed that the SEM for the 1280 °C sintered NAS2 sample had more void space in the structure at the lower magnification which could have been a result of sodium volatilization during high temperature sintering. This observation supports the low conductivity value for NAS2-1280 compared to that of the NAS2-1100 sample. Sintering temperatures have a major role on conductivity in NASICON samples [15,27]. It is evident from this systematic study that the temperature of 1100 °C for 12 h is ideal to get the highest conductivity of NASICON. Also, adding excess Na in the synthesis step is favored over adding excess of Na and P as the NAS2 sample showed the best conductivity of 1.13 mS cm^{-1} at 20 °C compared to the rest of samples. It is likely that the addition of both P and Na in NAS1 sample series had a major impact on decreasing their Na^+ ion conductivity.

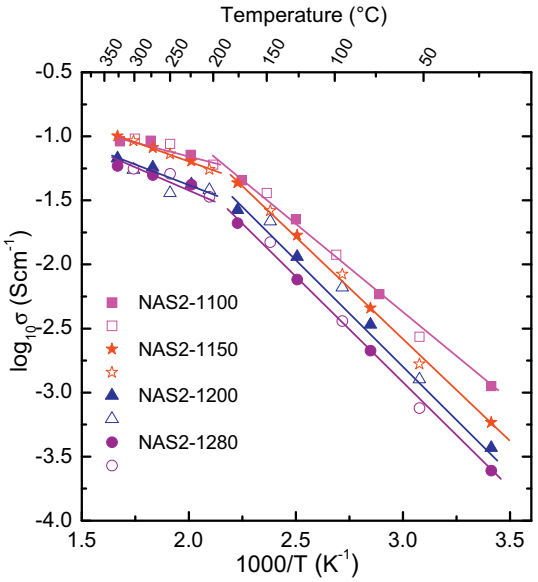

Fig. 8. Arrhenius plots of electrical conductivity of NASICON $Na_3Zr_2Si_2PO_{12}$ with excess Na (NAS2) at different sintering temperatures. The solid and open symbols represent the heating and cooling cycles, respectively.

Addition of excess sodium might be acting as a sintering aid in the case of NAS2 samples. However, the addition of excess P along with Na in NAS1 preparation might have created some non-conductive impurity phase at the grain-boundaries or which had not supported the sinterability of the NAS1 ceramics. More detailed study by varying the excess Na, Na and P while synthesizing $Na_3Zr_2Si_2PO_{12}$ may be needed to deeply understand the exact role of Na in enhancing the sample properties.

Table 3 summarizes the conductivity of NAS1 and NAS2 NASICONs at 20 °C with the activation energy calculated at two different temperature ranges 20–180 °C and 200–325 °C based on the plots of log σT vs. 1000/T along with the Archimedes density. The activation energy of NAS1 and NAS2 samples in the high temperature range is between 0.32 and 0.42 eV and the low temperature range is between 0.13 and 0.22 eV, respectively, which is similar to the reported literature values. It is known that $Na_3Zr_2Si_2PO_{12}$ undergoes a phase transition from monoclinic to rhombohedral after 200 °C [11]. The difference in slope may be attributed due to the corresponding phase transition. The conductivity and activation energy of $Na_3Zr_2Si_2PO_{12}$ NASICON from the literature is summarized along with the present results in Table 4 [12,14,21–24,26–36]. It shows that the synthesis conditions and sintering temperature has a great influence on the conductivity of the NASICON samples. The room temperature conductivity varied between 10^{-4} to 10^{-3} S cm^{-1} depending upon the choice of the synthesis method.

Finally, the electrochemical stability of NASICON at room temperature (25 °C) was tested using Na/NASICON/Na symmetrical cells employing galvanostatic cycling experiments. Fig. 9 shows the stripping-plating profiles of NAS2-1280 sample which was periodically charged and discharged for 30 min. A stable voltage of 0.01 V was maintained at 100 cycles for 100 h at a current density of 0.01 mA cm^{-2} indicating good interfacial stability.

4. Conclusions

The $Na_3Zr_2Si_2PO_{12}$ NASICON material was studied to understand the effects of excess Na and P, and Na alone, as well as the effect of sintering temperature on morphology and ionic conductivity. The samples synthesized using excess Na and sintered at 1100 °C (NAS1-1100) exhibited the highest conductivity of 1.13 mS cm^{-1} at 20 °C. It showed the lowest E_a of 0.32 and 0.13 eV which is calculated in the range of 20–180 and 200–325 °C, respectively. It is revealed that adding excess Na, instead of Na and P, helps improve the conductivity of NASICON materials. Also, increasing the sintering temperature from 1100 °C to 1280 °C reduces the ionic conductivity which could be due to the increase in volatilization at higher temperatures. However, the Archimedes density measurements showed that the density of all NASICON samples fall in the same range of ~3 g cm^{-3}. Our systematic studies show that a sintering temperature of 1100 °C for 12 h and adding excess Na salt (10 wt%) is ideal to obtain highly conducting, dense NASICON. A promising electrochemical stability was observed

Table 4
Conductivity, activation energy, and synthesis conditions of $Na_3Zr_2Si_2PO_{12}$ reported in literature.

σ of $Na_3Zr_2Si_2PO_{12}$ (S cm^{-1})	E_a (eV)	Synthesis condition	Ref.
0.2 (300 °C)	0.29	Solid-state synthesis (1250 °C/6–16 h)	[12]
1.5×10^{-3} (200 °C)	0.21	Sol-gel synthesis (1100 °C/2 h)	[28]
0.2 (350 °C)	–	Sol-gel synthesis (1000 °C/8 h)	[14]
1.03×10^{-3} (RT)	–	Solid-state synthesis (1280 °C/10 h)	[26]
2.2×10^{-3} (RT)	–	Molecular precursor method (900 °C/4 h)	[24]
6.4×10^{-4} (RT)	0.33	Sol-gel (1200 °C/0.5 h)	[23]
6.3×10^{-2} (300 °C)	0.14	Solid-state synthesis (1250 °C/20 h)	[29]
0.2 (300 °C)	0.29	Solid-state synthesis (1250 °C/15 h)	[30]
0.2 (300 °C)	0.20	Solid-state synthesis (1230 °C/24–48 h)	[31]
1.5×10^{-4} (25 °C); 0.11 (300 °C)	0.26	Sol-gel (1175 °C/1 h)	[32]
1.6×10^{-4} (25 °C); 0.13 (300 °C)	0.25	Sol-gel (1175 °C/16 h)	[32]
1×10^{-3} (25 °C)	–	Solution assisted solid-state synthesis (1250 °C/5 h)	[22]
8.9×10^{-4} (25 °C)	–	Pechini synthesis (1250 °C/5 h)	[22]
1.8×10^{-3} (25 °C)	–	Spark plasma sintering (1200 °C/0.5 h)	[33]
4×10^{-4} (RT)	0.36	Solid-state synthesis (1265 °C)	[21]
2.2×10^{-4} (RT)	–	Solid-state synthesis (1000 °C)	[27]
3.3×10^{-4} (RT)	–	Solid-state synthesis (1050 °C)	[27]
3.6×10^{-4} (RT)	–	Solid-state synthesis (1100 °C)	[27]
4.6×10^{-4} (RT)	–	Solid-state synthesis (1150 °C)	[27]
2.4×10^{-4} (RT)	–	Solid-state synthesis (1200 °C)	[27]
1.0×10^{-3} (RT)	0.38	Sol-gel (1200 °C)	[34]
7.5×10^{-4} (25 °C)		Sol-gel (1000 °C/1 h)	[35]
2.5×10^{-4} (RT)	0.41	Solid-state synthesis (1200 °C/overnight)	[36]
1.1×10^{-3} (25 °C)	0.32	Solid-state synthesis (excess Na, 1100 °C/12 h)	Present work
3.7×10^{-4} (25 °C)	0.37	Solid-state synthesis (excess Na and P, 1100 °C/12 h)	Present work

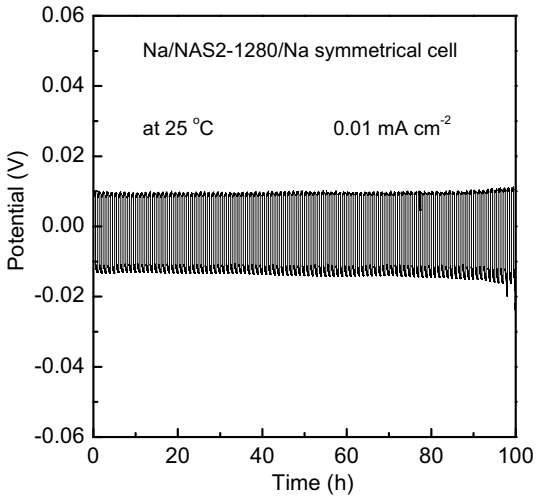

Fig. 9. Galvanostatic cycling of NAS2-1280 sample at 0.01 mA cm^{-2} at 25 °C using Na/NAS2-1280/Na symmetrical cell.

during the galvanostatic stripping-platting experiment for 100 cycles. This class of materials proves to be very useful in forming a basis to develop solid-state sodium-ion batteries for commercial secondary battery purposes. With future work including the addition of excess sodium, keeping sintering temperatures below the critical temperature for volatilization, and the introduction of other advanced technology into these devices, the solid-state sodium-ion battery will no doubt prove to be a disruptive technology for the market.

Acknowledgements

One of us (V. T.) would like to acknowledge the support from MITACS, a Canadian-profit national research organization, Geometric Energy Corporation, and the University of Calgary.

References

[1] S. Palakkathodi Kammampata, V. Thangadurai, Ionics 24 (3) (2018) 639.
[2] C. Vaalma, D. Buchholz, M. Weil, S. Passerini, Nat. Rev. Mater. 3 (2018) 18013.
[3] C. Zhou, S. Bag, V. Thangadurai, ACS Energy Lett. 3 (9) (2018) 2181.
[4] D. Kundu, E. Talaie, V. Duffort, L.F. Nazar, Angew. Chem. Int. Ed. 54 (11) (2015) 3431.
[5] A. Hayashi, K. Noi, N. Tanibata, M. Nagao, M. Tatsumisago, J. Power Sources 258 (2014) 420.
[6] A. Hooper, J. Phys. D. Appl. Phys. 10 (11) (1977) 1487.
[7] N. Tanibata, K. Noi, A. Hayashi, M. Tatsumisago, RSC Adv. 4 (33) (2014) 17120.
[8] M. Armand, J.M. Tarascon, Nature 451 (7179) (2008) 652.
[9] K.B. Hueso, M. Armand, T. Rojo, Energy Environ. Sci. 6 (3) (2013) 734.
[10] W. Zhou, Y. Li, S. Xin, J.B. Goodenough, ACS Cent. Sci. 3 (1) (2017) 52.
[11] H.Y.P. Hong, Mater. Res. Bull. 11 (2) (1976) 173.
[12] J.B. Goodenough, H.Y.P. Hong, J.A. Kafalas, Mater. Res. Bull. 11 (2) (1976) 203.
[13] W. Bogusz, F. Krok, W. Jakubowski, Solid State Ionics 803 (1983) 9–10.
[14] F. Qiu, Q. Zhu, X. Yang, Y. Quan, L. Sun, Sensors Actuators B Chem. 93 (1–3) (2003) 237.
[15] Z. Khakpour, Electrochim. Acta 196 (2016) 337.
[16] D. Chen, F. Luo, W. Zhou, D. Zhu, J. Alloys Compd. 757 (2018) 348.
[17] H. Park, M. Kang, Y.-C. Park, K. Jung, B. Kang, J. Power Sources 399 (2018) 329.
[18] F. Krok, Solid State Ionics 24 (1) (1987) 21.
[19] H. Park, K. Jung, M. Nezafati, C.S. Kim, B. Kang, ACS Appl. Mater. Interfaces 8 (2016) 27814.
[20] M. Guin, S. Indris, M. Kaus, H. Ehrenberg, F. Tietz, O. Guillon, Solid State Ionics 302 (2017) 102.
[21] R.O. Fuentes, F.M. Figueiredo, F.M.B. Marques, J.I. Franco, J. Eur. Ceram. Soc. 21 (6) (2001) 737.
[22] S. Naqash, Q. Ma, F. Tietz, O. Guillon, Solid State Ionics 302 (2017) 83.
[23] O. Bohnke, S. Ronchetti, D. Mazza, Solid State Ionics 122 (1) (1999) 127.
[24] P. Porkodi, V. Yegnaraman, P. Kamaraj, V. Kalyanavalli, D. Jeyakumar, Chem. Mater. 20 (20) (2008) 6410.
[25] W.H. Baur, J.R. Dygas, D.H. Whitmore, J. Faber, Solid State Ionics 935 (1986) 18–19.
[26] Y. Kim, H. Kim, S. Park, I. Seo, Y. Kim, Electrochim. Acta 191 (2016) 1.
[27] Y. Ruan, S. Song, J. Liu, P. Liu, B. Cheng, X. Song, V. Battaglia, Ceram. Int. 43 (10) (2017) 7810.
[28] F. Lalère, J.B. Leriche, M. Courty, S. Boulineau, V. Viallet, C. Masquelier, V. Seznec, J. Power Sources 247 (2014) 975.
[29] P. Pasierb, S. Komornicki, R. Gajerski, S. Koziński, P. Tomczyk, M. Rękas, J. Electroceram. 8 (1) (2002) 57.
[30] U. von Alpen, M.F. Bell, W. Wichelhaus, Mater. Res. Bull. 14 (10) (1979) 1317.
[31] W. Bogusz, F. Krok, W. Jakubowski, Phys. Status Solidi A 66 (2) (1981) K113.
[32] A. Ahmad, T.A. Wheat, A.K. Kuriakose, J.D. Canaday, A.G. McDonald, Solid State Ionics 24 (1) (1987) 89.
[33] J.-S. Lee, C.-M. Chang, Y.I. Lee, J.-H. Lee, S.-H. Hong, J. Am. Ceram. Soc. 87 (2) (2004) 305.
[34] H. Khireddine, P. Fabry, A. Caneiro, B. Bochu, Sensors Actuators B Chem. 40 (2) (1997) 223.
[35] Y. Noguchi, E. Kobayashi, L.S. Plashnitsa, S. Okada, J.-i. Yamaki, Electrochim. Acta 101 (2013) 59.
[36] M.L. Bayard, G.G. Barna, J. Electroanal. Chem. Interfacial Electrochem. 91 (2) (1978) 201.